

# Cooling and thermal stabilisation of Faraday rotators in the temperature range 300–200 K using Peltier elements

O.V. Palashov, I.B. Ievlev, E.A. Perevezentsev, E.V. Katin, E.A. Khazanov

**Abstract.** A new method for cooling and thermal stabilisation of Faraday rotators using Peltier elements is proposed and experimentally demonstrated. The scheme of thermal stabilisation of the magneto-optical elements ensures reliable operation of the device at the absorbed power  $\sim 2$  W, which corresponds to the transmitted laser radiation power 1.5 kW. The results of the work make it possible to predict high efficiency of this method at the laser power of tens of kilowatts.

**Keywords:** Faraday effect, permanent magnets, temperature stabilisation.

## 1. Introduction

Due to the rapid development of laser technology and the growth of the mean power of both cw and the repetitively pulsed laser radiation, there emerges an urgent problem to reduce the parasitic thermal effects (thermally induced depolarisation [1], thermal lensing [2]), arising in different optical elements through the laser radiation absorption. One of such devices is a Faraday rotator (FR) with rather high absorption ( $10^{-3}$  cm $^{-1}$  [3, 4]) in the magneto-optical elements (MOEs). There exist several approaches to the problem of reduction of thermally induced depolarisation in MOEs of a FR. One of them is based on the idea of subtraction of the phase incursion by replacing one MOE, rotating the polarisation plane through  $45^\circ$ , with two MOEs, each providing a  $22.5^\circ$  rotation, with a reciprocal optical element between them [1, 5]. The distortions, introduced by the first element are partially compensated when passing the second one.

Another approach implies an increase in the magnetic field by using either the magnetic circuits [2] or the magnets with a nonorthogonal magnetisation axis [6] in the construction of the magnetic system (MS), which allows the reduction of the MOE length and, therefore, of the absorbed heat. The third approach is to divide the MOE into several thin disks, cooled through the optical surface [7, 8]. This geometry provides an essential reduction of the transverse temperature gradient. The fourth approach implies the cooling of the paramagnetic MOE up to the temperature of liquid nitrogen [9–11]. Since the Verdet constant in paramagnetic materials is inversely

proportional to the temperature [9, 12], and the magnitude of the magnetic field for some ferromagnetic alloys grows with the cooling of the magnetic system, it is also possible to reduce essentially the length of the MOE. In this case, the heat conductivity of the crystal is additionally improved [13] and the cold depolarisation in it decreases [9]. However, this method is rather expensive and labour-consuming. Essential reduction of the MOE temperature is possible by means of a simpler method using Peltier elements (PEs). In the present paper we report the experimental results on reducing the temperature to  $\sim 200$  K using two commercially available PEs.

All mentioned methods allow one to reach the cw laser power up to  $P_L \sim 1$  kW (and more), keeping the degree of FR isolation high ( $\sim 30$  dB). However, even at lower levels of the power the first two methods, presently being the most widespread, suffer from an essential drawback. The degree of isolation, the main characteristic of a FR, becomes time-dependent because of unavoidable and relatively high heat generation in the MOE. Indeed, the characteristic MOE length in a high-power FR is  $\sim 1$  cm, so that the released heat power in the MOE at the kilowatt level of the laser power is  $\sim 1$  W. The released heat, as a rule, is lead to the MS through bushings. As a result, due to the temperature dependence of the Verdet constant of the MOE and the magnetic properties of the MS, the angle of rotation, provided by the FR, decreases with time. This reduces the isolation degree of the device. The characteristic transient time during which the system comes to a quasi-stationary regime, in which the angle of rotation is practically constant, depends on many factors (heat extraction from the MOE, geometry and construction of the MS) and may amount to tens of minutes. Using PEs the thermal stabilisation of the MOE is possible with the prescribed temperature independent of the amount of heat release. This can be convenient when the FR is used in a scheme with tunable laser power.

## 2. Cooling and thermal stabilisation using Peltier elements

The scheme of thermal stabilisation, presented in Fig. 1, consists of the Peltier element (1), thermal sensor (3), and control unit (2). The heat extraction from the outer face of the PE is implemented by means of the radiator (5) cooled with water. The inner face is attached to the copper bushing (6), at the end of which the MOE (7) placed inside the magnetic system of the FR is mounted.

The Peltier element operation principle is based on the thermoelectric effect, i.e., release or absorption of heat when the electric current passes through a contact of two different conductors (a pair) [14]; the number of pairs determines the power of the PE. In the used PE (TB-38-1.0-1.5CHR,

O.V. Palashov, I.B. Ievlev, E.A. Perevezentsev, E.V. Katin, E.A. Khazanov Institute of Applied Physics, Russian Academy of Sciences, ul. Ul'yanova 46, 603950 Nizhnii Novgorod, Russia; e-mail: palashov@appl.sci-nnov.ru, eperevezentsev@gmail.com

Received 31 May 2011  
Kvantovaya Elektronika 41 (9) 858–861 (2011)  
Translated by V.L. Derbov

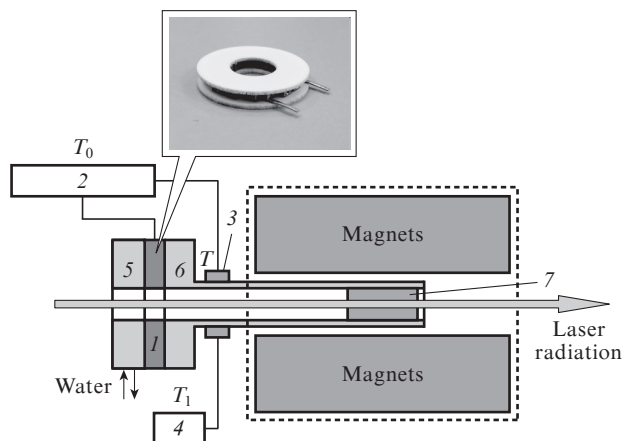


**Figure 1.** Scheme of thermal stabilisation: (1) Peltier element; (2) PE control unit; (3) and (4) heat sensors; (5) water-cooled radiator; (6) copper bushing; (7) MOE.

KRIOTERM, Saint-Petersburg), comprising 38 pairs of contacts, the maximal heat extraction power is 9 W. The control unit (2) is the PE power supply that provides the control of the heat extraction power and allows setting (by means of a variable resistor) the target temperature  $T_0$ . The 2N5551 silicon transistor in the diode regime, having a linear temperature dependence of voltage ( $2.6 \text{ mV deg}^{-1}$ ), was used as a heat sensor (3).

The thermal stabilisation is implemented as follows. The signal from the heat sensor (3), measuring the temperature  $T$  of the bushing, enters the control unit and is compared with the temperature  $T_0$ . If the condition  $T > T_0$  is valid, the rectangular voltage pulses with the given amplitude  $U_0$  are applied to the PE. The duration  $\tau$  of the pulses can vary in the range  $(0.1-0.5)\tau_0$  ( $\tau_0 \sim 1 \text{ ms}$ ) and is determined by the temperature difference  $T - T_0$ . The result of operation of the thermal stabilisation scheme was analysed by the temperature readout  $T_1$  of the heat sensor (4) (Fig. 1). Note, that  $T_1$  is not the temperature of the MOE itself, but the temperature of the point of the copper bushing  $\sim 3 \text{ cm}$  far from the MOE, because it is technically impossible to place the heat sensor (with linear size  $\sim 5 \text{ mm}$ ) inside the MS of the FR (the gap  $\sim 0.5 \text{ mm}$ ). However, according to the performed calculations, the temperature difference between the heat sensor (4) attaching point and the MOE location ( $\sim 0.1^\circ\text{C}$ ) does not exceed the error of the temperature measurement.

The cooling scheme of the optical element is presented in Fig. 2. The optical element (6) was indium-soldered to the copper plate (5) cooled using the PE (4). The 'hot' side of the PE (4) (FROST-74, KRIOTERM, Saint Petersburg, maximal temperature difference 74 K, extracted heat power 65 W) was cooled by means of the PE (3) (DRIFT-0.6, maximal temperature difference 69 K, extracted heat power 220 W), whose 'hot' side was cooled with the water radiator (1). The PE power was continuously adjustable by the control unit. Using only one of the mentioned PEs we managed to achieve cooling in the range from 235 to 240 K. Further reduction of the optical element temperature requires the use of two PEs. Essential reduction of the optical element temperature simply by increasing the number of PEs seems impossible, because the temperature difference between the hot and the cold faces of the element tends to zero at lowering its mean temperature. The optical element was placed in the vacuum chamber (2) to

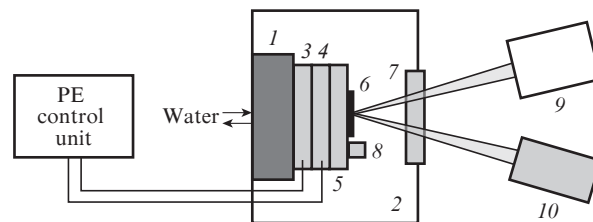


**Figure 2.** Scheme of the optical element cooling: (1) water radiator; (2) vacuum chamber; (3) and (4) Peltier elements; (5) copper plate; (6) optical element; (7) AR-coated window; (8) heat sensor; (9) 'heating' laser; (10) absorber.

prevent condensation on its surface. The optical element was heated with the cw radiation of the laser (9) through the AR-coated window (7). The temperature of the copper plate was measured by means of the heat sensor (8).

### 3. Experimental results

Schematic diagram of the experimental setup used to study the thermal stabilisation of the FR is presented in Fig. 3. The radiation from the 1076-nm, 330-W single-mode fibre ytterbium laser (1) (IPG Photonics) was used as both the heating and the probing radiation simultaneously. The linearly polarised radiation after the spar wedge (2) passed through the MOE of the FR (3), thermally stabilised by the PE (4). Then, the main part of the radiation power was reflected by the highly reflecting mirror (8), passed through the MOE again and after reflection from the polariser (7) arrived at the absorber (6). This scheme allows a double increase in the maximal heating of the MOE. A part of the laser radiation, transmitted through the mirror (8), was additionally attenuated at the silica wedge (5), passed through the Glan prism (9), installed on the limbed table, and was detected with the CCD-camera (10). Heating of the MOE causes the decrease in the Verdet constant and, therefore, the reduction of the rotation angle, introduced by the FR and, hence, the increase in the radiation power of the depolarised component  $P_d$ , detected with the CCD-camera.

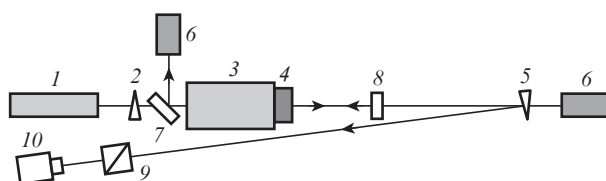


**Figure 3.** Schematic diagram of the experimental setup: (1) ytterbium fibre laser; (2) spar wedge; (3) Faraday rotator; (4) thermal stabilisation system; (5) silica wedge; (6) absorber; (7) polariser; (8) mirror; (9) Glan prism; (10) CCD-camera.

The experiment was carried out in two stages. First, the heating of the MOE by the laser radiation, registered with the temperature meter (4) (Fig. 1), was implemented with the thermal stabilisation scheme being switched off. At the second stage the regime of thermal stabilisation of the MOE was investigated. The control unit was set to provide the target temperature, satisfying the condition  $T_0 < T_c$  ( $T_c \sim 20^\circ\text{C}$ ). The control unit generated the voltage  $U(t)$ , applied to the PE, as

a result of which the MOE temperature  $T_1$  was decreased and stabilised. The laser radiation with the power  $P_L$  arrived at the FR (Fig. 3) at the moment of time  $t = 0$ .

Three Faraday rotators were experimentally studied. First, we studied the FR designed according to the traditional scheme, i.e., with a single MOE made of the magneto-optical MOS-04 glass (the absorption  $\alpha = 10^{-3} \text{ cm}^{-1}$ , the length  $L = 15 \text{ mm}$ , the diameter  $d = 10 \text{ mm}$ ) [3, 4] and with the PE of the round shape. The results of the measurements are presented in Fig. 4 (triangles). When the scheme of thermal stabilisation is switched off ( $\Delta$ ) and  $P_L = 330 \text{ W}$  (the power of heat production  $\sim 0.5 \text{ W}$ ) the MOE was heated by  $7^\circ\text{C}$  in 30 min. The switched-on thermal stabilisation scheme with the target temperature  $T_0 = 20.5^\circ\text{C}$  ( $\blacktriangle$ ) essentially reduced the heating during the same 30 min:  $T_1 = 21 \pm 0.5^\circ\text{C}$ , and with the target temperature  $18^\circ\text{C}$  ( $\blacktriangle$ ) the MOE temperature was stabilised at  $T_1 = 18.5 \pm 0.5^\circ\text{C}$ .

The second experimental sample was a wide-aperture FR, operating according to the scheme with the depolarisation compensation [1, 5]. Two crystals of terbium–gallium garnet (TGG) were used for a MOE ( $d = 30 \text{ mm}$ , the total length  $L = 22 \text{ mm}$ ,  $\alpha = 2.7 \times 10^{-3} \text{ cm}^{-1}$ , the power of heat generation  $\sim 2 \text{ W}$  at  $P_L = 330 \text{ W}$ ), placed at the ends of copper bushings at the opposite sides of the FR. The temperature was stabilised using the TV-31-1.4-1.15 PE of the square shape supplied by the same manufacturer (the maximal extracted heat power  $\sim 19 \text{ W}$ ). Two PTs were attached to each bushing contrariwise to each other with respect to the symmetry axis. The choice of the other type of the PE is dictated by the absence of commercially produced PEs with the inner hole larger than 20 mm. Without thermal stabilisation the MOE was heated by  $5^\circ\text{C}$  during 30 min (Fig. 4, white squares), and with thermal stabilisation ( $T_0 = 17^\circ\text{C}$ ) the MOE temperature was constant during the whole time of observation (Fig. 4, grey squares).

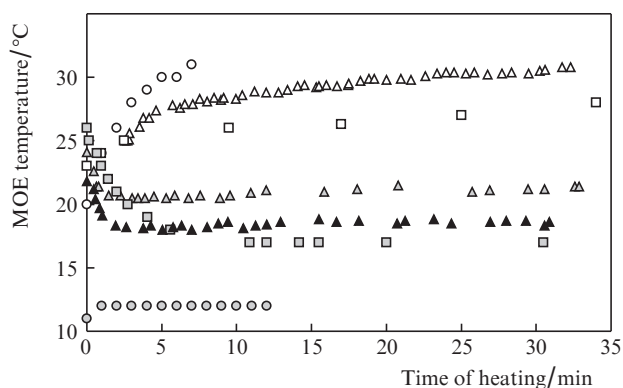


**Figure 4.** MOE temperature versus time of heating in the FR with the round PE (triangles), rectangular PE (squares) and without water-cooled PE (circles) in the regime without thermal stabilisation (white dots) and with thermal stabilisation (dark dots).

In the cases considered above the MOE was thermally stabilised using water-cooled PEs. Water cooling of the PEs was chosen for the reasons of convenience. This choice was not a matter of principle, and water cooling could be replaced with air cooling. However, the implementation of MOE thermal stabilisation is possible without a PE, using, e.g., the water cooling directly. The corresponding experiment was carried out with a FR built according to the scheme with the compensation of thermal depolarisation at the light aperture 20 mm.

The MOE consisted of two TGG crystals (the total length  $L = 20 \text{ mm}$ ,  $\alpha = 1.7 \times 10^{-3} \text{ cm}^{-1}$ , the heat generation power  $\sim 2 \text{ W}$  at  $P_L = 612 \text{ W}$ ). The faces of copper bushings (Fig. 1) were cooled using water radiators (the water temperature  $\sim 10^\circ\text{C}$ ) from two sides of the FR casing.

In the regime without thermal stabilisation (Fig. 4, white circles) the MOE is quickly heated (by  $10^\circ\text{C}$  during 5 min). The decrease in the Verdet constant with the temperature rise due to the MOE heating leads to a decrease in the FR rotation angle. Figure 5 shows the experimental dependence of the deviation  $\Delta\varphi$  of the polarisation plane rotation angle, registered using the Glan prism and the CCD-camera (Fig. 3). For this purpose, the Glan prism is rotated through a certain angle  $\theta$ , at which the value of the depolarisation, measured with the CCD-camera, is minimal in the regime without thermal stabilisation (Fig. 5, white circles), and with thermal stabilisation (Fig. 5, grey circles). In this case, the transverse beam structure has a pronounced Maltese-cross shape with the symmetry axes rotated through the angle  $\theta/2$ . In the thermal stabilisation regime upon switching on the laser the MOE temperature slightly increased during the first minute and then became stable (Fig. 4, grey circles). From the data on the temperature variation (Fig. 4) with the temperature dependence of the Verdet constant taken into account we can calculate  $\Delta\varphi$  in the regimes without thermal stabilisation (Fig. 5, white triangles) and with thermal stabilisation (Fig. 5, grey triangles). Figure 5 also shows the time dependence of the degree of isolation  $I = 10 \lg(P_L/P_d)$  for the measured angle of the polarisation plane rotation  $\Delta\varphi$  (Fig. 5, white squares).

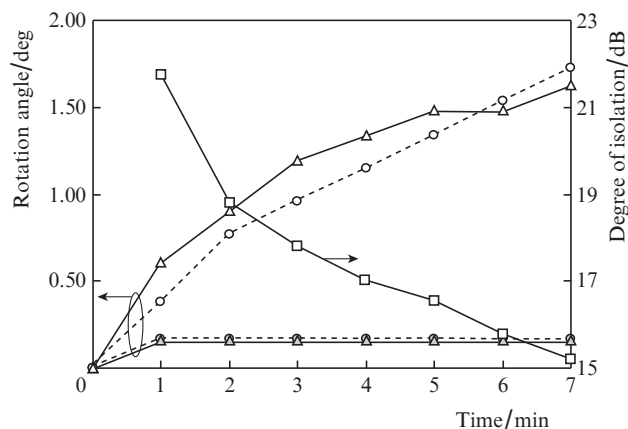


**Figure 5.** Experimental (circles) and calculated (triangles) dependences of the deviation of the rotation angle  $\theta$  of the polarisation plane in the regime without thermal stabilisation (white dots) and with thermal stabilisation (grey dots), together with the calculated dependence of the degree of isolation  $I$  (squares) on the time of MOE heating by 612-W laser radiation.

The model experiments on cooling by means of PEs were carried out with the disk-shaped active element (6) (Fig. 2) made of a 400- $\mu\text{m}$ -thick Yb:YAG crystal (with the Yb content of 10%) 10 mm in diameter. One side of the element had an AR coating, while the other had no AR coating. The heating of the optical element occurs through the AR-coated using the cw radiation of the diode laser (9) (JOLD-75-CPXF-2P, JENOPTIK Laserdiode, Germany) at the well-absorbed wavelength 940 nm. With the laser switched off, the temperature of the copper plate (5) decreased down to 210 K. Switching on

the laser with the total power 70 W (which corresponds to the absorbed power of 25 W) lead to the increase in the minimal temperature, at which the optical element can be thermally stabilised, to 240 K. With an intermediate thermal load the dependence of the minimal temperature on the absorbed power may be considered linear.

According to Ref. [11], cooling down to 210 K by using shorter MOEs and improving the thermo-optical constants allows a double increase in the radiation power passing through the FR. The absorbed power for the FRs, considered above, is  $\sim 4$  W. Such thermal generation does not practically affect the temperature difference, created by the pair of FRs used.

## 4. Conclusions

The paper demonstrates an efficient way of cooling and thermal stabilisation of magneto-optical elements of Faraday rotators by means of Peltier elements. Stable operation of the FR at room temperatures and the level of absorbed power  $\sim 2$  W in the MOE made of TGG have been experimentally demonstrated. Using purer crystals (at present  $\alpha < 7 \times 10^{-4} \text{ cm}^{-1}$  for commercially available TGG crystals) will allow increasing the cw laser power to nearly  $\sim 1.5$  kW.

Using two PEs we have obtained experimentally the thermal stabilisation and the cooling of the optical element in the temperature range 300–210 K. Cooling down to 210 K yields a double increase in the laser radiation power (up to 3 kW). The model experiment on cooling and thermal stabilisation of the Yb:YAG optical element in the temperature range 300–240 K allows one to expect efficient operation of the PE at the heat release power up to 25 W, which corresponds to the power of laser radiation  $\sim 20$  kW.

Thermal stabilisation of the MOE at room temperatures was accomplished using two methods, namely, cooling with Peltier elements and with water. The cooling by running water is the simplest way, but it suffers from one drawback: the target temperature  $T_0$  cannot be controlled. The use of a closed contour of water cooling requires stabilisation of  $T_0$ , e.g., by using a chiller. As shown by our experiments, thermal stabilisation of MOE using the Peltier elements is more simple, cheap and no less reliable.

## References

1. Khazanov E.A. *Kvantovaya Elektron.*, **29**, 59 (1999) [*Quantum Electron.*, **29**, 894 (1999)].
2. Mukhin I.B., Voitovich A.V., Palashov O.V., Khazanov E.A. *Opt. Commun.*, **282**, 1969 (2009).
3. Zarubina T.V., Malshakov A.N., Pasmanik G.A., Potemkin A.K. *Opt. Zh.*, **64**, 11 (1997).
4. Zarubina T.V., Petrovskii G.T. *Opt. Zh.*, **59**, 48 (1992).
5. Voitovich A.V., Katin E.V., Mukhin I.B., Palashov O.V., Khazanov E.A. *Kvantovaya Elektron.*, **37**, 471 (2007) [*Quantum Electron.*, **37**, 471 (2007)].
6. Mironov E.A., Voitovich A.V., Palashov O.V. *Kvantovaya Elektron.*, **41**, 71 (2011) [*Quantum Electron.*, **41**, 71 (2011)].
7. Mukhin I.B., Khazanov E.A. *Kvantovaya Elektron.*, **34**, 973 (2004) [*Quantum Electron.*, **34**, 973 (2004)].
8. Yasuhara R., Kawashima T., Furukawa H., et al. *Proc. Int. Symp. «Topical Problem of Nonlinear Wave Physics»* (St. Petersburg–N. Novgorod, 2005) p. 135.
9. Zhelezov D.S., Voitovich A.V., Mukhin I.B., Palashov O.V., Khazanov E.A. *Kvantovaya Elektron.*, **36**, 383 (2006) [*Quantum Electron.*, **36**, 383 (2006)].
10. Zhelezov D.S., Mukhin I.B., Palashov O.V., Khazanov E.A., Voitovich A.V. *IEEE J. Quantum Electron.*, **43**, 451 (2007).
11. Zhelezov D.S., Zelenogorskii V.V., Katin E.V., Mukhin I.B., Palashov O.V., Khazanov E.A. *Kvantovaya Elektron.*, **40** (3), 276 (2010) [*Quantum Electron.*, **40** (3), 276 (2010)].
12. Davis J.A., Bunch R.M. *Appl. Opt.*, **23**, 633 (1984).
13. Slack G.A., Oliver D.W. *Phys. Rev. B*, **4**, 592 (1971).
14. Seeger K. *Semiconductor Physics* (Berlin: Springer, 1999).